

Michael addition-driven synthesis of cytotoxic palladium(II) complexes from chromone thiosemicarbazones: Investigation of anticancer activity through *in vitro* and *in vivo* studies

Jebiti Haribabu,^{a,*} Nithya Balakrishnan,^b Srividya Swaminathan,^c Dorothy Priyanka Dorairaj,^b Mohammad Azam,^d Mohamed Kasim Mohamed Subarkhan,^e Yu-Lun Chang,^f Sodio C. N. Hsu,^{f,g} Pavel Štarha,^h Ramasamy Karvembu^{b,*}

^a*Facultad de Medicina, Universidad de Atacama, Los Carreras 1579, 1532502 Copiapo, Chile*

^b*Department of Chemistry, National Institute of Technology, Tiruchirappalli 620015, India*

^c*Center for Computational Modeling, Chennai Institute of Technology (CIT), Chennai 600069, India*

^d*Department of Chemistry, College of Science, King Saud University, Riyadh 11451, Saudi Arabia*

^e*The First Affiliated Hospital, Key Laboratory of Combined Multi-Organ Transplantation, Ministry of Public Health, School of Medicine, Zhejiang University, Hangzhou, 310003, PR China*

^f*Department of Medicinal and Applied Chemistry, Drug Development and Value Creation Research Centre, Kaohsiung Medical University, Kaohsiung 80708, Taiwan*

^g*Department of Medical Research, Kaohsiung Medical University Hospital; Department of Biotechnology, Kaohsiung Medical University, Kaohsiung 80708, Taiwan*

^h*Department of Inorganic Chemistry, Faculty of Science, Palacky University Olomouc, 17 Listopadu 12, 77146 Olomouc, Czech Republic*

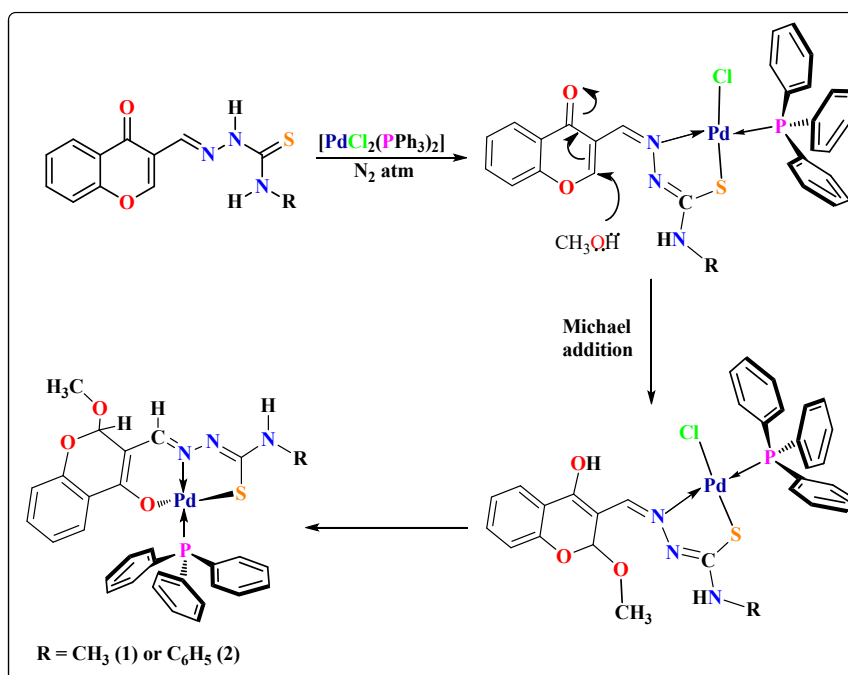
Corresponding authors E-mail id: haribabusiri970@gmail.com (J.H.), kar@nitt.edu (R.K.)

Table of contents

Materials and methods	S3
Scheme S1. Proposed mechanism for the formation of new Pd(II) complexes 1 and 2 based on previously reported mechanism for complex 3	S3
Results and discussion	S4
Fig. S1 UV-Visible spectra of the complexes.	S4
Fig. S2 FT-IR spectrum of complex 1 .	S5
Fig. S3 FT-IR spectrum of complex 2 .	S5
Fig. S4 ^1H NMR spectrum (500 MHz) of complex 1 in CDCl_3	S6
Fig. S5 $^{13}\text{C}\{^1\text{H}\}$ NMR spectrum (125 MHz) of complex 1 in CDCl_3	S6
Fig. S6 DEPT-135 NMR spectrum (125 MHz) of complex 1 in CDCl_3	S7
Fig. S7 $^{31}\text{P}\{^1\text{H}\}$ NMR spectrum (202 MHz) of complex 1 in CDCl_3	S7
Fig. S8 ^1H NMR spectrum (500 MHz) of complex 2 in CDCl_3	S8
Fig. S9 $^{13}\text{C}\{^1\text{H}\}$ NMR spectrum (125 MHz) of complex 2 in CDCl_3	S8
Fig. S10 DEPT-135 NMR spectrum (125 MHz) of complex 2 in CDCl_3	S9
Fig. S11 $^{31}\text{P}\{^1\text{H}\}$ NMR spectrum (202 MHz) of complex 2 in CDCl_3	S9
Fig. S12 Effect of Pd(II) complexes 1-3 and cisplatin against normal (Vero) cells. Data were calculated by mean \pm S.D. with three replications.	S10
References	S10

Materials and methods

Chemicals obtained from commercial suppliers were used as received and were of analytical grade. The melting points were measured on a Lab India instrument and are uncorrected. Elemental analyses were carried out using a PerkinElmer instrument. FT-IR spectra were obtained as KBr pellets using a Nicolet-iS5 spectrophotometer. UV-Visible spectra were recorded using a Shimadzu-2600 spectrophotometer. NMR spectra were recorded in deuterated chloroform by using TMS as an internal standard on a Bruker 500 MHz spectrometer. X-ray diffraction data collection and corrections for complex **3** were done at 113(2) K with an APEX K_{α} diffractometer using graphite monochromated MoK_{α} ($k = 0.71073 \text{ \AA}$) radiation. The structural solution was obtained readily using XT/XS in APEX2^{1,2} and refined by full matrix least squares on F^2 using Olex2. The used (2*E*)-2-[(4-oxo-4*H*-chromen-3-yl)methylidene]hydrazinocarbothioamide-based chromone TSCs, bearing the terminal methyl (SVSHL1), phenyl (SVSHL2) or cyclohexyl (SVSHL3) substituent, were prepared according the formerly reported method.³



Scheme S1. Proposed mechanism for the formation of new Pd(II) complexes **1** and **2** based on previously reported mechanism for complex **3**.³

Results and discussion

Preliminary characterization using UV-Visible and FT-IR spectroscopy

UV-Visible spectra of the complexes were recorded in the wavelength range of 200-800 nm in DMSO. The absorption bands at 257 and 272 nm for complex **1** and 259 and 273 nm for complex **2** were specified to $\pi \rightarrow \pi^*$ and $n \rightarrow \pi^*$ transitions, respectively.⁴⁻⁶ Complex **1** exhibited ligand to metal charge transfer transitions (LMCT) in the regions 368 and 381 nm. Similarly, the bands at 365 and 386 nm for complex **2** were related to LMCT.⁴ FT-IR spectra of complexes **1** and **2** showed terminal N-H stretching frequency at 3365 or 3368 cm^{-1} , respectively. The complexes showed an absorption band at 1480 cm^{-1} due to the azomethine group. The bands at 1330 and 1332 cm^{-1} in the spectra of complexes **1** and **2**, respectively, were assigned to $\nu(\text{C-O})$. A band due to $\nu(\text{C-S})$ was observed at 1171 (**1**) or 1174 (**2**) cm^{-1} . In addition, a band appeared at 1574 (**1**) or 1573 (**2**) cm^{-1} was assigned to $\nu(\text{C=C-O})$. The presence of PPh_3 in the complexes was confirmed by the appearance of bands at 1434, 1095 and 760 cm^{-1} .^{4,6}

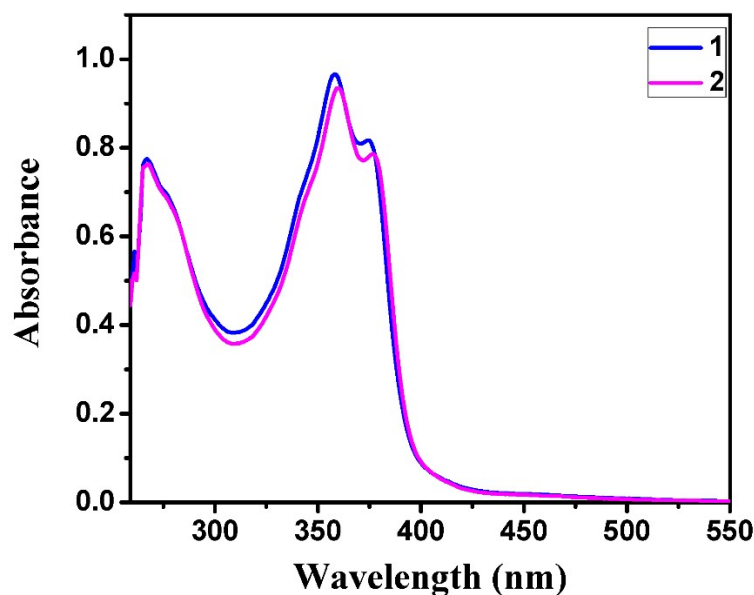


Fig. S1 UV-Visible spectra of the complexes.

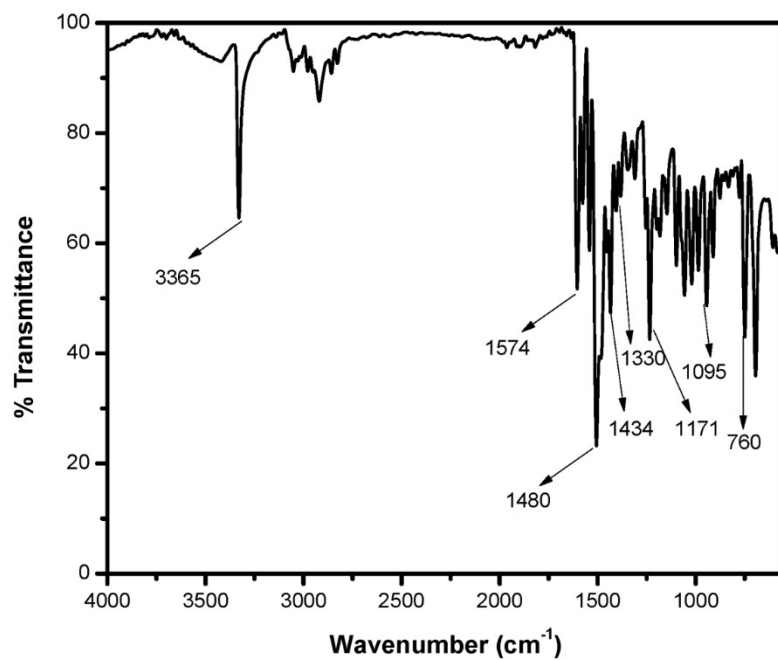


Fig. S2 FT-IR spectrum of complex 1.

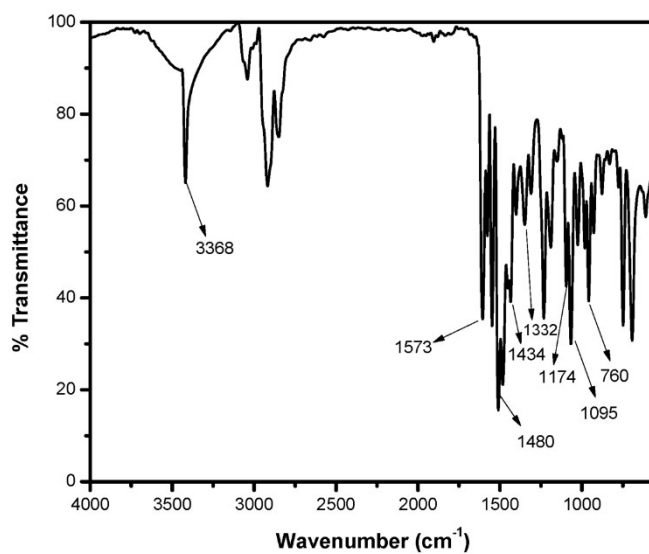


Fig. S3 FT-IR spectrum of complex 2.

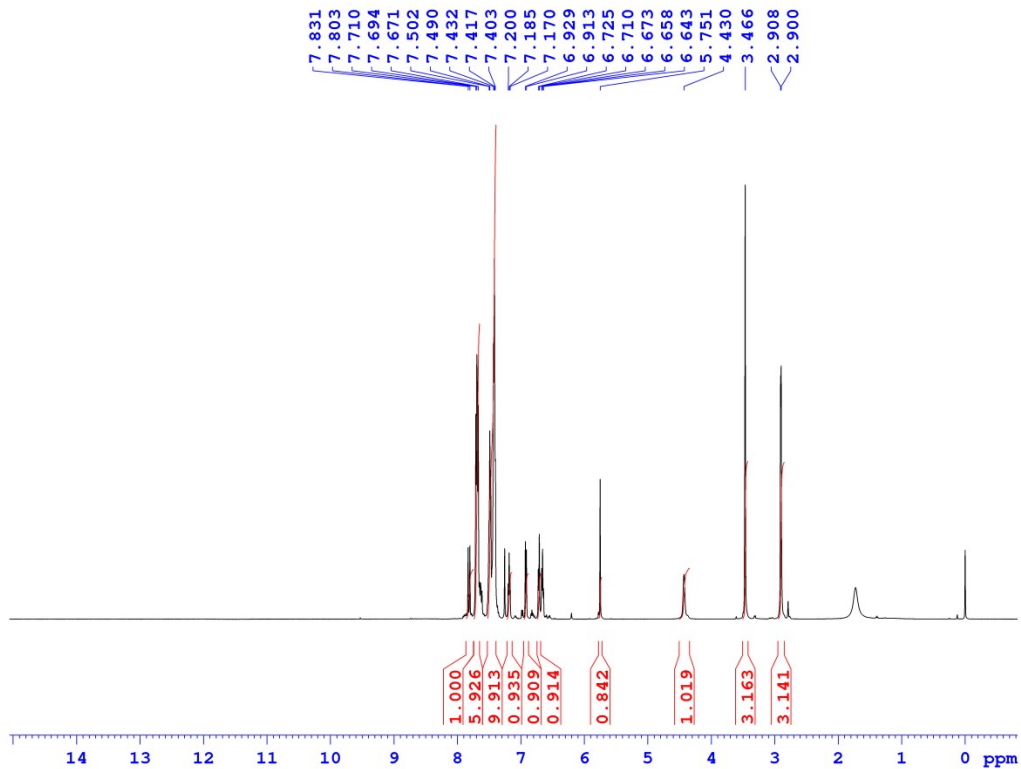


Fig. S4 ^1H NMR spectrum (500 MHz) of complex **1** in CDCl_3 .

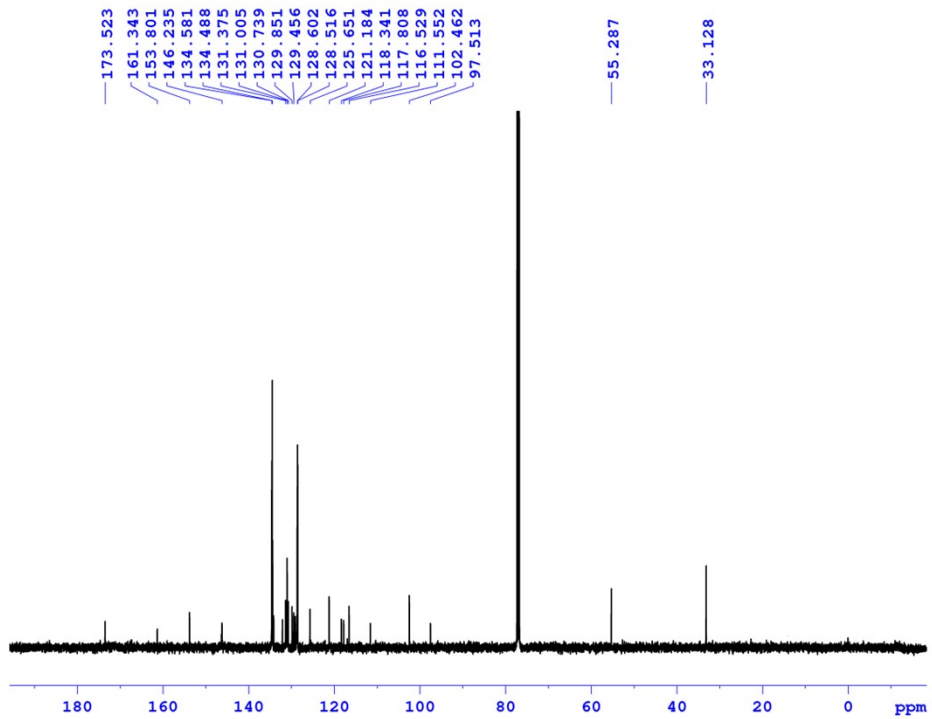


Fig. S5 $^{13}\text{C}\{^1\text{H}\}$ NMR spectrum (125 MHz) of complex **1** in CDCl_3 .

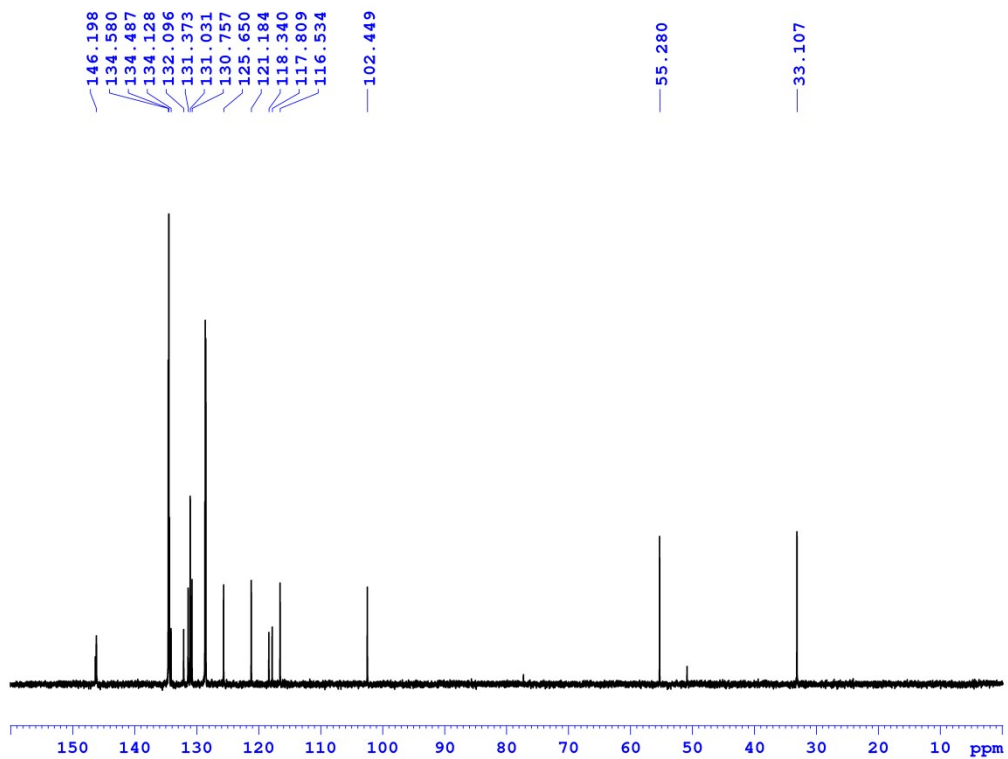


Fig. S6 DEPT-135 NMR spectrum (125 MHz) of complex **1** in CDCl_3 .

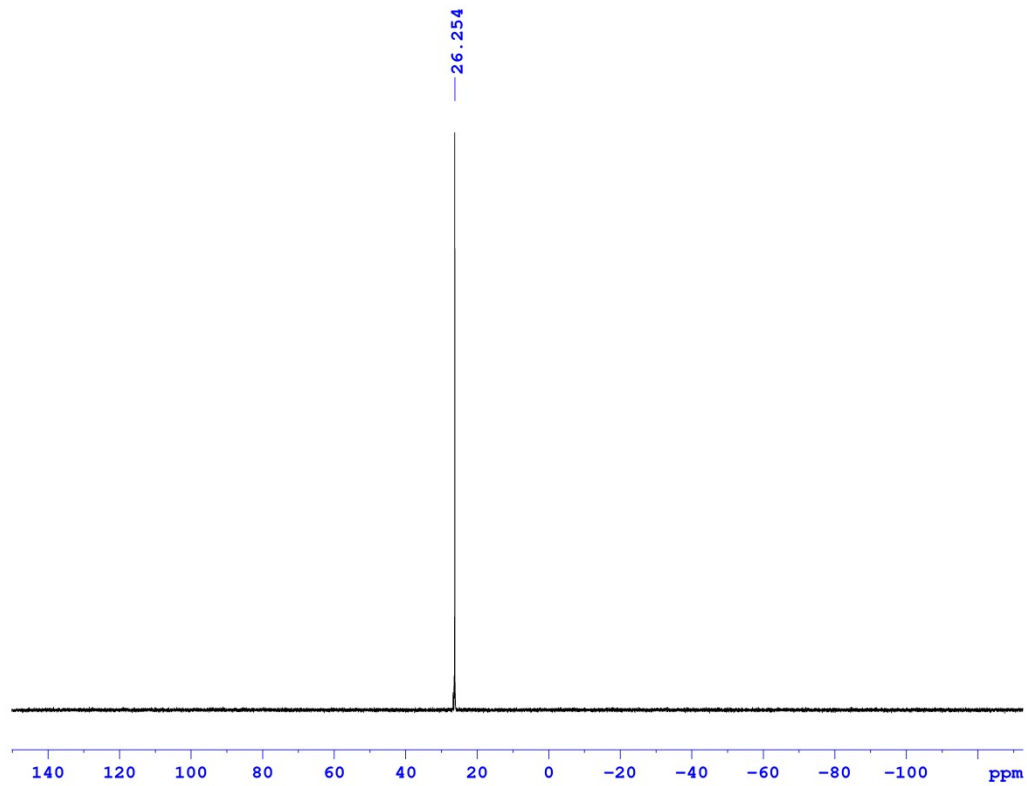


Fig. S7 $^{31}\text{P}\{^1\text{H}\}$ NMR spectrum (202 MHz) of complex **1** in CDCl_3 .

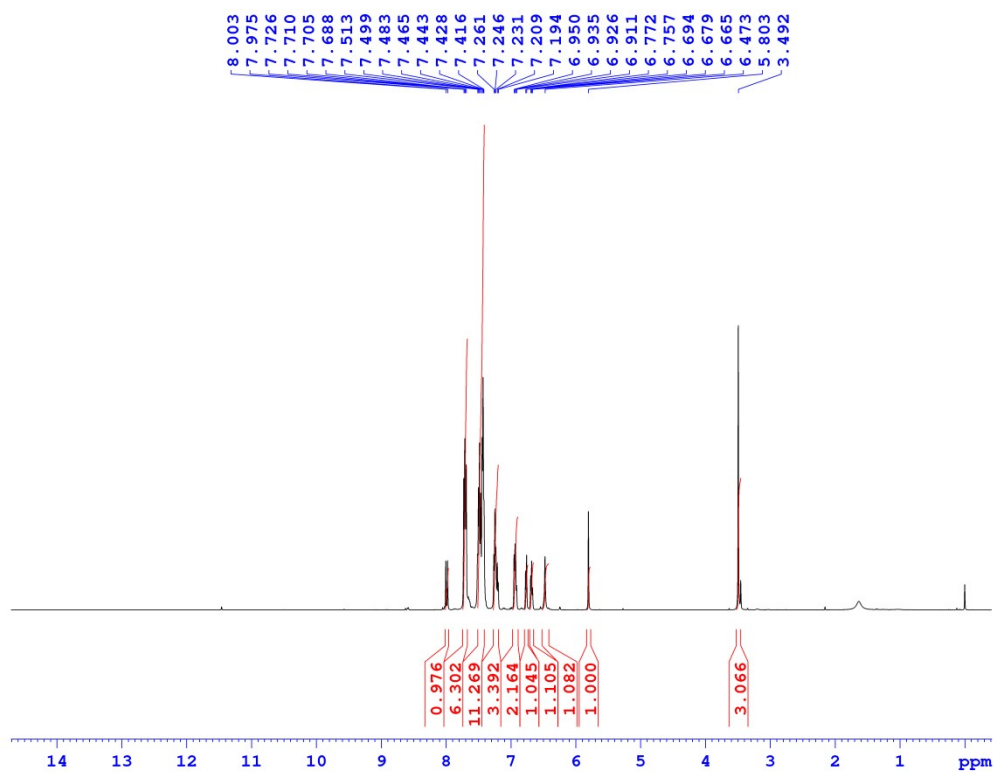


Fig. S8 ^1H NMR spectrum (500 MHz) of complex **2** in CDCl_3 .

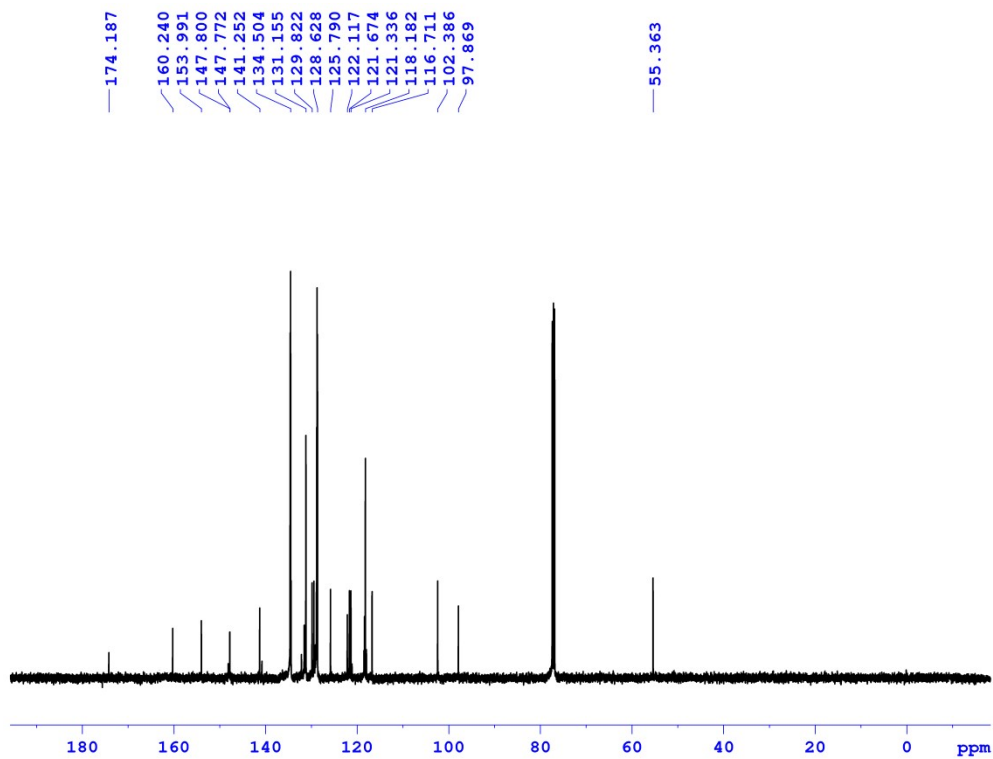


Fig. S9 $^{13}\text{C}\{^1\text{H}\}$ NMR spectrum (125 MHz) of complex **2** in CDCl_3 .

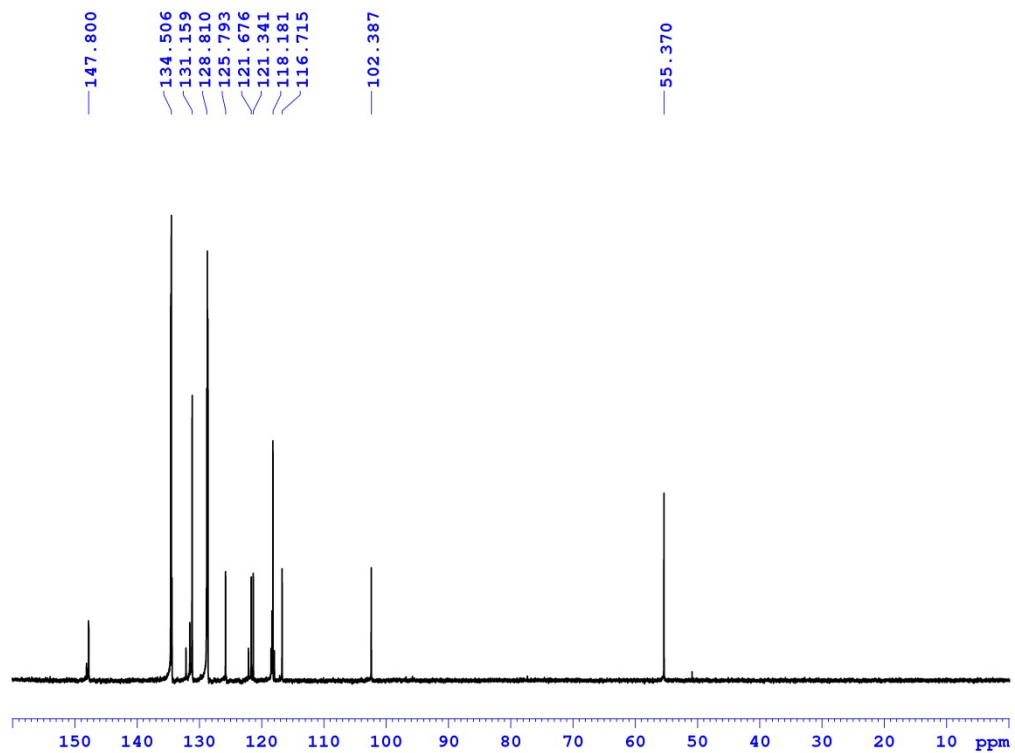


Fig. S10 DEPT-135 NMR spectrum (125 MHz) of complex **2** in CDCl₃.

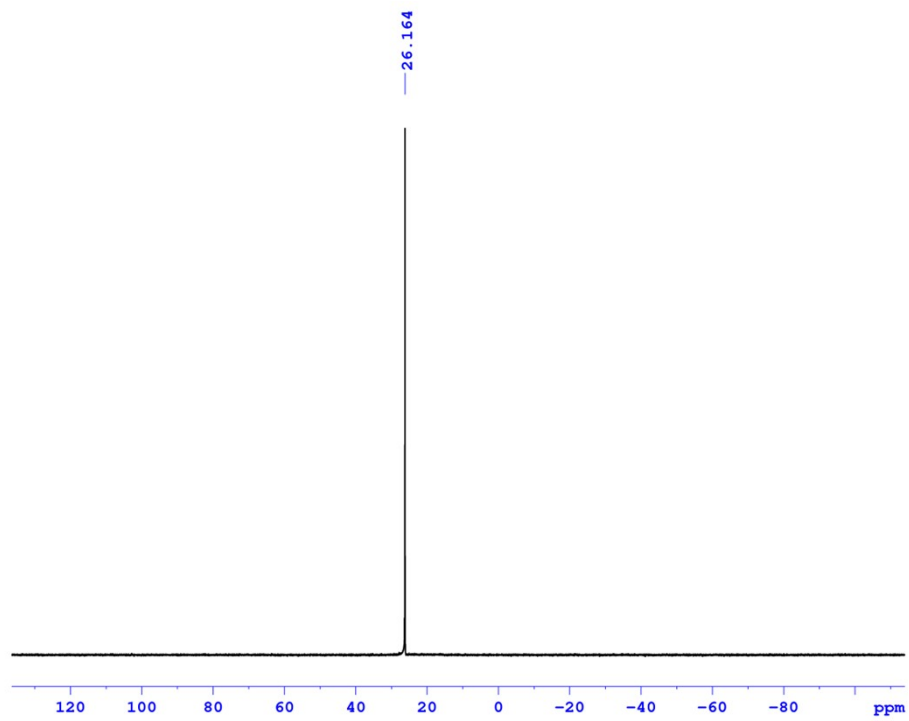


Fig. S11 ³¹P{¹H} NMR spectrum (202 MHz) of complex **2** in CDCl₃.

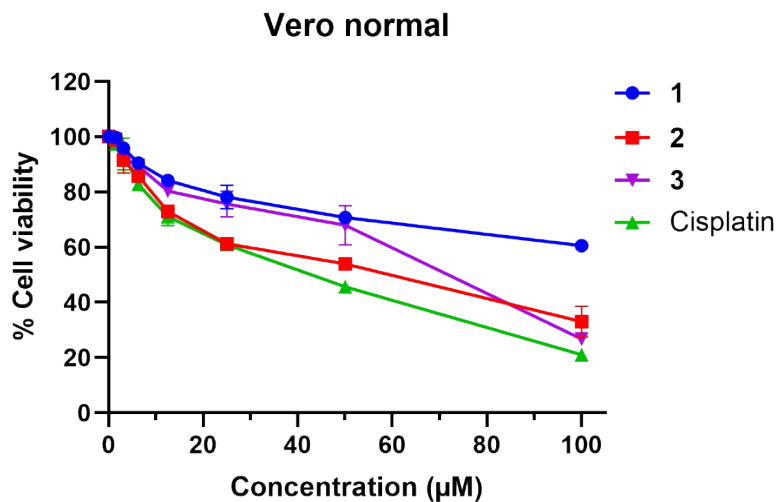


Fig. S12 Effect of Pd(II) complexes **1-3** and cisplatin against normal (Vero) cells. Data were calculated by mean \pm S.D. with three replications.

References

1. APEX2 “*Program for Data Collection and Integration on Area Detectors*”, Bruker AXS Inc., 5465 East Cheryl Parkway, Madison, WI 53711–5373, USA.
2. Sheldrick, G. M. “*TWINABS (version 2008/1): Program for Absorption Correction for Data from Area Detector Frames*”, University of Göttingen, 2008.
3. J. Haribabu, S. Srividya, D. Mahendiran, D. Gayathri, V. Venkatramu, N. Bhuvanesh and R. Karvembu, *Inorg. Chem.*, 2020, **59**, 17109–17122.
4. N. Balakrishnan, J. Haribabu, A. K. Dhanabalan, S. Swaminathan, S. Sun, D. F. Dibwe, N. Bhuvanesh, S. Awale and R. Karvembu, *Dalton Trans.*, 2020, **49**, 9411–9424.
5. J. Haribabu, C. Balachandran, M. M. Tamizh, Y. Arun, N. S. P. Bhuvanesh, S. Aoki and R. Karvembu, *J. Inorg. Biochem.*, 2020, **205**, 110988.
6. A. Shanmugapriya, R. Jain, D. Sabarinathan, G. Kalaiarasi, F. Dallemer and R. Prabhakaran, *New J. Chem.*, 2017, **41**, 10324–10338.